(10) 20011??72

THREE-DIMENSIONAL UPWARD FLAME SPREADING IN PARTIAL-GRAVITY BUOYANT FLOWS

Kurt R. Sacksteder, NASA Glenn Research Center, Cleveland OH
Ioan I. Feier, Hsin-Yi Shih, and James S. T'ien, Case Western Reserve Univ., Cleveland OH

Introduction

Reduced-gravity environments have been used to establish low-speed, purely forced flows for both opposed- and concurrent-flow flame spread studies. Altenkirch's group obtained space-based experimental results and developed unsteady, two-dimensional numerical simulations of opposed-flow flame spread including gas-phase radiation, primarily away from the flammability limit for thin fuels, but including observations of thick fuel quenching in quiescent environments[1]. T'ien's group contributed some early flame spreading results for thin fuels both in opposed flow[2,3] and concurrent flow[4] regimes, with more focus on near-limit conditions. T'ien's group also developed two- and three-dimensional numerical simulations of concurrent-flow flame spread incorporating gas-phase radiative models,[5,6,7,8] including predictions of a radiatively-induced quenching limit reached in very low-speed air flows. Radiative quenching has been subsequently observed in other studies of combustion in very low-speed flows including other flame spread investigations,[9] droplet combustion and homogeneous diffusion flames, and is the subject of several contemporary studies reported in this workshop.

Using NASA aircraft flying partial-gravity "parabolic" trajectories, flame spreading in purely-buoyant, opposed-flow (downward burning) has been studied.[10] These results indicated increases in flame spread rates and enhanced flammability (lower limiting atmospheric oxygen content) as gravity levels were reduced from normal Earth gravity, and were consistent with earlier data obtained by Altenkirch using a centrifuge.[11]

In this work, experimental results and a three-dimensional numerical simulation of upward flame spreading in variable partial-gravity environments were obtained including some effects of reduced pressure and variable sample width. The simulation provides physical insight for interpreting the experimental results and shows the intrinsic 3-D nature of buoyant, upward flame spreading. This study is intended to link the evolving understanding of flame spreading in purely-forced flows to the purely-buoyant flow environment, particularly in the concurrent flow regime; provide additional insight into the existence of steady flame spread in concurrent flows; and stimulate direct comparisons between opposed- and concurrent-flow flame spread. Additionally, this effort is intended to provide direct practical understanding applicable to fire protection planning for the habitable facilities in partial gravity environments of anticipated Lunar and Martian explorations.

Experiments

Upward flame spreading was observed in reduced-pressure air environments in normal-gravity and in partial-gravity environments using the GIFFTS test apparatus[10] with slight modifications. Fig.1 shows the test apparatus. Fuel samples were a thin cellulosic tissue, trade name "Kimwipes," used by others.[2,3,4,10] An improved, repeatable sample-drying procedure was developed using a hot-air gun. Test pressures between 0.2-0.4 atmospheres were established using primary standard, precision mixtures of 21% O_2, balance N_2. Flight tests were performed

onboard the NASA KC-135 aircraft providing partial-gravity environments of 0.1, 0.16, and 0.38 g/g_{earth}. Chamber pressure and 3-axis accelerations were recorded by the GIFFTS computer. Conventional video and a FSI Inc. Prism DS IR camera with a flame filter at 3.8μm (to reject emissions from H_2O, CO_2) were used to image the solid surface.

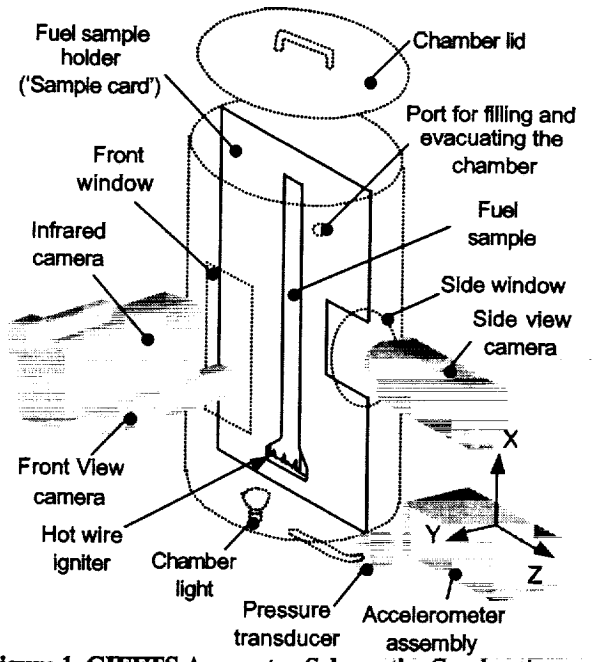

Figure 1. GIFFTS Apparatus Schematic: Combustion chamber (27 liter), thin stainless-steel sample-holder cards with 1,2 and 4 cm wide gaps for fuel exposure on both sides, conventional video imaging of the fuel surface and edge, infrared camera for imaging the fuel surface through a 3.8μm flame reject filter, a pressure transducer and 3-axis accelerometer. Samples are ignited using a resistively heated Kanthol alloy wire (approximately 100J ignition energy). An embedded computer controls the experiment operation and data acquisition sequence.

Numerical Flame Spread Simulation

A 3-dimensional model developed to simulate steady laminar flame spread and extinction over a thin solid fuel in low-speed forced concurrent flows[8] was modified to simulate purely buoyant flow in partial-gravity and reduced-pressure environments. For the gas phase, full three-dimensional, steady, laminar Navier-Stokes equations for conservation of mass, momentum, energy and species (O_2, N_2, CO_2, H_2O and fuel vapor) were solved. Gas-phase reactions were modeled using one-step, second-order Arrhenius kinetics. The thermally thin solid model consists of continuity and energy equations with a surface radiative loss (ε=0.92) whose solutions provide the boundary conditions for the gas phase. Fuel pyrolysis is modeled as a one-step, zeroth-order Arrhenius process; manifested as shrinking fuel thickness. Gas-phase radiation was neglected at this stage of the buoyant model development.

Results of Experiments and the Numerical Simulation

A more detailed summary of the experimental and numerical results can be found in reference 12. Figure 2 shows a comparison of a visible flame and the computed gas-phase reaction rates from the numerical simulation. The computed flames are longer than the experimental counterparts, but the shape of the experimental flames are well reproduced by the simulation. Experimentally, short flame shapes were steady and regular; longer flames exhibited oscillating tips and irregular shapes. Figure 3 shows a comparison of an image of the pyrolyzing fuel and the computed fuel thickness. In both cases, the downstream pyrolysis front is pointed, suggesting the three dimensional nature of the flames. Figure 4 shows comparisons between IR camera indications of fuel surface temperature and the computed values. The centerline temperature profiles in Fig. 4c are qualitatively similar; but the computed surface temperatures are higher than the equivalent blackbody temperature indicated by the camera detector. Surface emissivity less than unity would increase the temperatures indicated by the camera data, but the actual emissivity of partially pyrolyzed Kimwipes at elevated temperatures is not known. Figure 5 shows a comparison of measured and experimental pyrolysis and flame lengths for 2 cm wide samples burning at different gravity levels at 0.27 atm pressure. While the trend with gravity level is the same, the computed lengths are consistently longer than the measured values. (A pre-

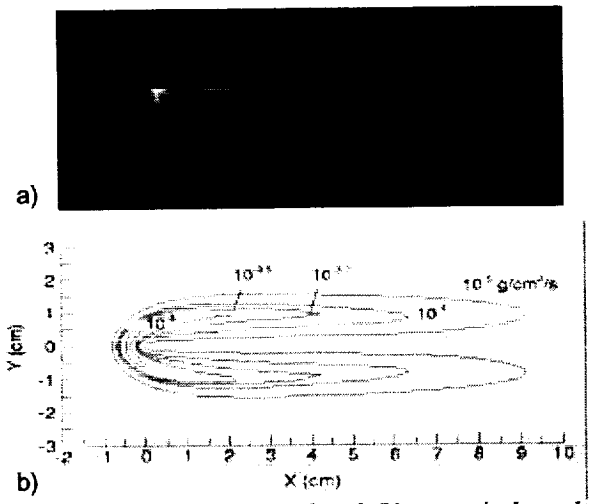

Figure 2. (a) Experimental and (b) numerical results showing upward flame spread over thin fuel samples 2cm wide in 0.16 g/g_{earth} (g vector toward the left) and 0.27 atm pressure. Computed fuel reactivity contours shown are values integrated over the 3D flame width. Values of approximately 10^{-4} $g/cm^2/s$ correspond to the visible flame length.

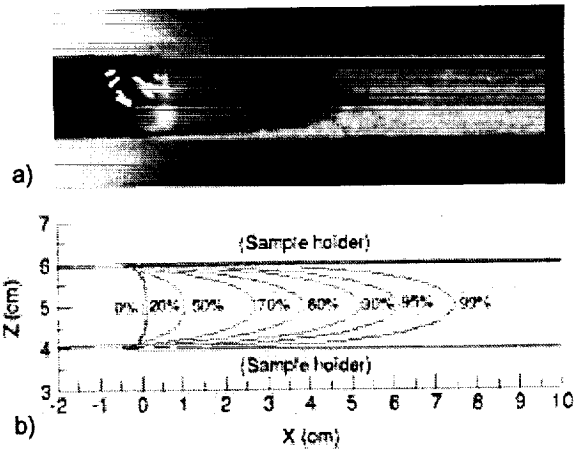

Figure 3. (a) Experimental and (b) numerical results showing the visible degradation of the fuel compared to computed fuel thickness contours for upward flame spread over thin fuel samples 2cm wide in 0.16 g/g_{earth} (g vector toward the left) and 0.27 atm pressure. Computed fuel thicknesses of approximately 95% of the unburnt fuel correspond to the onset of visible discoloration.

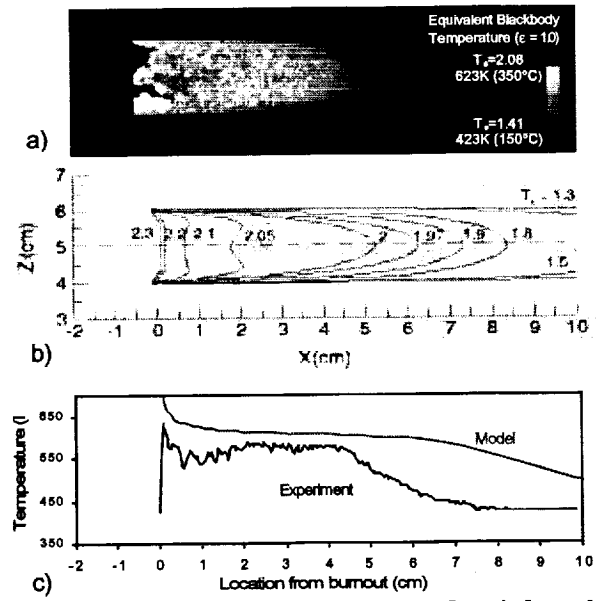

Figure 4. Comparison of (a) fuel surface infra-red image, (b) computed dimensionless fuel surface temperatures, and (c) centerline fuel surface temperatures from (a) and (b) for 2-cm wide fuel burning in 0.16 g/g_{earth}, and 0.27 atm pressure. The IR camera reports equivalent blackbody temperatures, and its sensitivity limits the lowest detectable temperature to 423K.

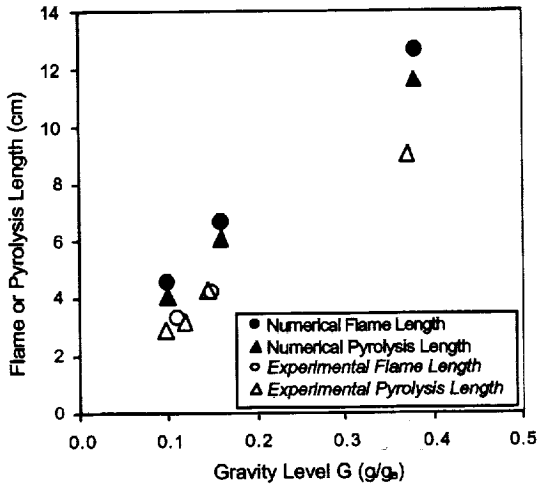

Figure 5 Comparison of experimental and computed flame and pyrolysis lengths of 2 cm wide samples burning at 0.27 atm pressure in various gravity levels.

vious 2-D flame-spread simulation,[6] showed that including flame radiation shortens the flame and pyrolysis lengths in low-speed flow with little affect on spread rates.) Figure 6a shows computed results in a plane perpendicular to the fuel surface. Downstream, the temperature contours are nearly parallel to the fuel. In this buoyancy-driven case, flow is induced by density gradients and accelerates inside the flame from 10cm/s just upstream of the flame to 60 cm/s downstream. In purely forced-flow, the downstream flames and streamlines diverge from the fuel,[4,5] unless the flow is confined by a

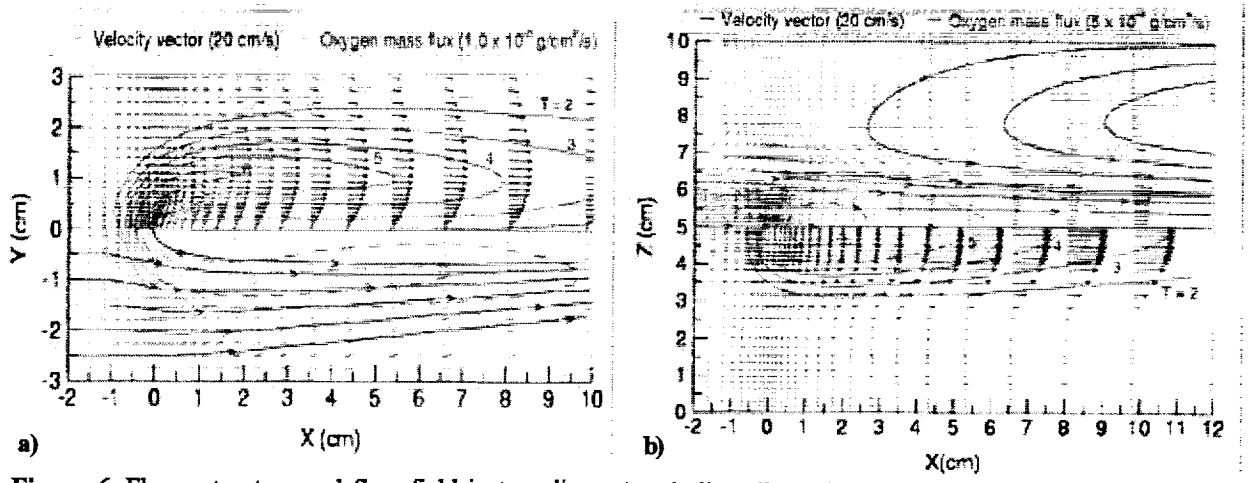

Figure 6. Flame structure and flow field in two-dimensional slices through an upward spreading flame over a 2cm wide sample in 0.16g/g_{earth}, 0.27atm pressure, oriented **a)** perpendicular to fuel surface and **b)** parallel to and 1 cm above the fuel surface. In a), the top half of the image shows velocity vectors, non-dimensional temperature (T=1 is 300K). Bottom half shows streamlines, oxygen mass flux vectors, and fuel reaction rate contours (10^{-3}, 10^{-4}, 10^{-5} g/cm^3/s from smallest to largest contour.) In b), the data presentation is reversed. Note the characteristic buoyant velocity profile in a), with the local peak inside the flame, and in b) the lateral entrainment of air and the substantial diffusion of oxygen across the streamlines.

small wind tunnel.[7,8] Figure 6b shows computed results in a plane parallel to and offset by 1cm from the fuel surface. In the purely buoyant flow, the gas accelerates throughout the length of the flame, entraining air from the sides and pulling the streamlines toward the central plane. Flow recirculation occurs beside the flame. Oxygen diffuses into the flame from the side at fluxes comparable to the convective oxygen stream. The entrainment, recirculation and lateral diffusion could not be observed in a two-dimensional simulation. Although not shown here, the computed flame spread rates closely predicted corresponding experimental rates. The simulation predicted significantly wider flammability limits than were observed in the experiments. As forced-flow simulations have shown,[7] flame and pyrolysis lengths shrink and flammability limits narrow when gas-phase radiation is included in the flame spread simulations. Better agreement between the experimental and simulation results can be expected once the existing gas radiation model is coupled to the 3D buoyant code. Despite this limitation, the model shows agreement with the flame behavior trends that were experimentally observed.

References

1. Sacksteder, K.R., ESA SP-454, 1st Int. Symp. Microg. Res. & Appl., Sorrento, Italy, (2000).
2. Olson, S.L., Ferkul, P.V., and T'ien, J.S., Proc. Combust. Inst. Vol. 22, pp.1213-1222 (1988).
3. Olson, S.L., Comb. Sci. Tech., Vol. 76, pp. 233-249, (1991).
4. Grayson, G.D., Sacksteder, K.R., Ferkul, P.V., T'ien, J.S., Microg. Sci. Tech. VII-2 (1994).
5. Ferkul, P.V., and T'ien, J.S., Vol. 99, pp. 345-370 (1994).
6. Jiang, C.B., T'ien, J.S. and Shih, H.Y., Proc. Combust. Inst. Vol. 26, pp.1353-1360 (1996).
7. Shih, H.Y. and T'ien, J.S., AIAA 97-0236, 35th Aerospace Sciences Meeting, (1997).
8. Shih, H.Y. and T'ien, J.S. Proc. Combust. Inst. Vol. 28, to appear.
9. Honda, L. K. and Ronney, P. D., Proc. Combust. Inst. Vol. 28, to appear.
10. Sacksteder, K.R., and T'ien, J.S., Proc. Combust. Inst., Vol. 25, pp. 1685-1692 (1994).
11. Altenkirch, R.A., Eichorn R., Shang, P.C., Combust. Flame, Vol. 37, pp. 71-83 (1980).
12. Feier, I.I., Shih, H-Y, Sacksteder, K.S., and T'ien, J.S., AIAA-2001-0466, 39th Aerospace Sciences Meeting, (2001).